JOURNAL OF BACTERIOLOGY, Feb. 1997, p. 1246–1252 Vol. 179, No. 4
0021-9193/97/$04.00+0

Further Characterization and In Situ Localization of Chain-Like Aggregates of the Gliding Bacteria *Myxococcus fulvus* and *Myxococcus xanthus*

ANJA FREESE,[1]† HANS REICHENBACH,[2] AND HEINRICH LÜNSDORF[1]*

Gesellschaft für Biotechnologische Forschung mbH, Abteilung Mikrobiologie,[1] and Abteilung Mikrobielle Sekundärstoffe,[2] D-38124 Braunschweig, Germany

Received 18 September 1996/Accepted 9 December 1996

For the first time, chain-like aggregates, called "strands," have been enriched from crude cell wall preparations of liquid-grown vegetative cells of two strains of *Myxococcus xanthus*. These strands are highly isomorphic to macromolecular structures, previously described for *Myxococcus fulvus* (Lünsdorf and Reichenbach, J. Gen. Microbiol. 135:1633–1641, 1989). The strands are morphologically composed of ring elements, consisting of six or more peripheral protein masses and possibly three small central masses. The ring elements are linked by two parallel strings of filamentous proteins, called elongated elements, which keep the ring elements at a constant distance. The overall dimensions of the ring elements are 16.6 ± 1.0 nm ($n = 55$) for *M. xanthus* Mx x48 and 16.4 ± 1.5 nm ($n = 37$) for *M. xanthus* DK 1622. The distance between the ring elements, as a measure of the length of the elongated elements, is 16.6 ± 1.1 nm ($n = 59$) for strain Mx x48 and 15.5 ± 0.6 nm ($n = 41$) for strain DK 1622. Characteristically, the strands and oligomeric forms thereof show a strict association with the outer membrane. In situ studies of freeze-fractured cells of *M. fulvus* showed ring elements, isomorphic to those described for *M. xanthus*, within the periplasm; they appeared in parallel rows just below the outer membrane but not in direct contact with the cytoplasmic membrane. A three-dimensional model summarizes the morphological data. It is hypothesized that the chain-like strands, as building blocks of a more complex belt-like continuum, represent the peripheral part of the gliding machinery, which transforms membrane potential energy into mechanical work.

Gliding motility is defined as bacterial translocation in contact with a surface and in the absence of flagella. This kind of motility is widespread among prokaryotes, particularly those of the gram-negative cell type, and may be found with at least 6 out of 10 phylogenetic groups (31, 32, 37). Gliding bacteria are able to colonize relatively dry habitats like soil, rotten wood, and other decaying organic material. But gliding motility clearly has ecological implications. Thus, gliding bacteria are often found associated with primary microbial communities, e.g., in the rhizosphere (1, 33). Their ecological importance as predators on the population density of cyanobacteria in a freshwater environment is obvious, since *Phormidium luridum* was shown to be effectively lysed by *Myxococcus* (6, 7, 11). Only by its efficient gliding motility *Thioploca* sp., a sulfur bacterium, which forms 5-cm-thick mats along the continental shelf of the Pacific coast of Peru and Chile at a length of 3,000 km, is able to link the marine nitrogen and sulfur cycles by transport of nitrate over 10 to 15 cm vertically from the top into the hydrogen sulfide-containing sediment. This transport is about 40 times faster than transport by diffusion (16). Gliding phototrophic cyanobacteria, for instance, are able to move within a day to that stratum in the microbial mats that offers optimum light intensity (8).

The characteristic ability of myxobacteria to aggregate and when starving to organize themselves into species-specific fruiting bodies is inevitably linked to gliding motility, as well as signal transduction, the basis of intercellular communication (for reviews, see references 15, 21, 22, and 36).

However, in spite of many efforts the structural basis of the gliding apparatus has not yet been discovered and characterized, although several hypotheses have been proposed (for more details on the physical models of gliding motility, the reader may refer to recent excellent reviews: references 3, 4, 8, 13, 18, 27, and 35).

In 1989, we could show for the first time by high-resolution electron microscopy ultrastructural details of a complex macromolecular structure which we regard to be part of the gliding machinery of *Myxococcus fulvus* (25). Negatively stained, isolated chain-like "strands" and highly organized aggregates of them ("ribbons" arranged in a "belt") could be seen. These aggregates showed a striking conformational flexibility that could well translate into a constriction wave. The superstructure showed a stringent ultrastructural correlation with a distinct helical surface pattern of the vegetative cell.

The present work further substantiates our previous observations from freeze-fracture studies of the in situ state of the strands, and it extends the evidence of this apparatus to another member of the genus *Myxococcus*, *M. xanthus*. A dichotomous model of the machinery of gliding motility, viz., energy transfer from the cytoplasmic membrane and energy transformation into mechanical work at the outer membrane by conformational changes of the strands, is discussed.

MATERIALS AND METHODS

Bacterial growth and harvest. *M. fulvus* Mx f65-9 and *M. xanthus* DK 1622 were grown as described by Lünsdorf and Reichenbach (25). The cells were harvested during the late logarithmic phase by centrifugation at 8,000 × *g* at 4°C for 15 min and were washed twice in HEPES-NaCl buffer at a buffer/sediment volume ratio of 5:1 at 4°C (HEPES [pH 7.5], 10 mmol/liter; $CaCl_2$, 1 mmol/liter; benzamidine, 1 mmol/liter; after pH adjustment with 10 mol of NaOH per liter

* Corresponding author. Mailing address: GBF, Abteilung Mikrobiologie, Mascheroder Weg 1, D-38124 Braunschweig, Germany. Phone: (49) 531-6181495. Fax: (49) 531-6181411. E-mail: lunsdorf@gbf-braunschweig.de.

† Present address: Institut für Immunologie der Universität Kiel, D-24105 Kiel, Germany.

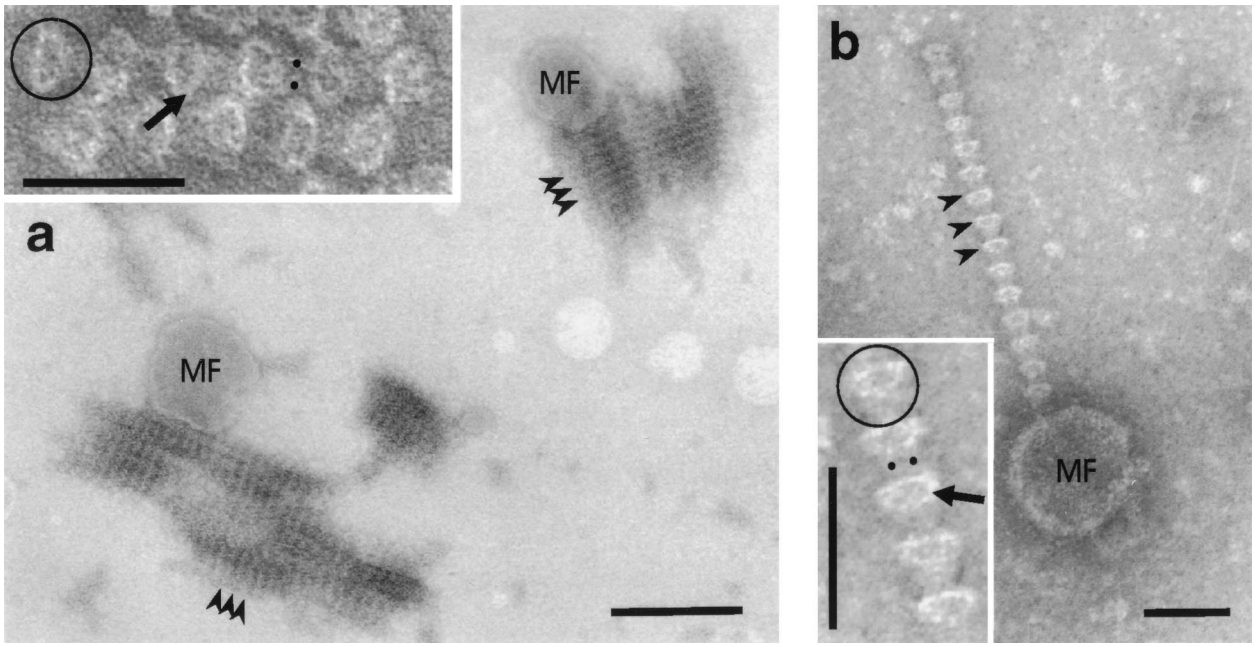

FIG. 1. Negatively stained chain-like aggregates, so-called strands, of *M. xanthus* vegetative cells after mechanical disruption. (a) Survey of patches of aggregated strands from *M. xanthus* Mx x48. These superstructures appear associated with membrane fragments (MF). The characteristic periodic spacing of ring elements is indicated by massive arrowheads. Inset: Details of two strand fragments. The ring element of the strand is encircled, and the central fibrillar elongated elements are indicated by dots. Notice the opposite orientation of the ring elements within both strands. Bar, 150 nm; (inset, 30 nm). (b) Single strand fragment of *M. xanthus* DK1622, associated with a membrane fragment (MF). The ring elements (arrowheads) are standing oblique to the plane of the carbon support. Inset: Ring elements (circle) and central elongated elements (dots) are shown at higher magnification; arrow indicates the spoke-like central mass. Bar, 50 nm (inset, 30 nm).

the buffer was made 0.75 mmol of 2-mercaptoethanol per liter and 100 mol of NaCl per liter). The cells of *M. xanthus* Mx x48 were obtained frozen and were kindly supplied by Irschik (Gesellschaft für Biotechnologische Forschung mBH [GBF], Braunschweig, Germany). The cells were washed with HEPES-NaCl buffer at a buffer/sediment volume ratio of 5:1 at 4°C.

Isolation of chain-like aggregates (strands). Washed suspensions of cells in HEPES-NaCl buffer were disintegrated by two passages through a French pressure cell (Aminco, Urbana, Ill.) at 56.34 MPa (= 8,000 lb/in^2). Cell debris was incubated with DNase (0.1 mg/ml final concentration) at 4°C for 15 min, followed by sedimentation at 17,000 × *g* for 30 min at 4°C. The supernatant was discharged, and the cell wall pellet was resuspended in HEPES-NaCl buffer at a buffer/sediment volume ratio of 10:1 and stored at 4°C. The purified cell wall fragments were treated with lysozyme (1 mg/ml) for 90 min at 30°C, followed by sedimentation at 17,000 × *g* at 4°C for 30 min. The sediment was thoroughly resuspended by repeated intensive pumping with a Pasteur pipette in HEPES-NaCl buffer. Isopycnic gradients from 50 to 60% (wt/vol) sucrose, buffered with HEPES-NaCl, were underlaid with a cushion of 65% (wt/vol) sucrose in HEPES-NaCl buffer and covered with steps of 40 and 30% (wt/vol) sucrose in HEPES-NaCl buffer. The volume ratios of individual steps from high to low sucrose densities were 1:7:1:1. The gradients were loaded with 0.8 to 1.0 ml of the sample with 4.4 to 5.0 mg of total protein. Centrifugation was done for 20 h at 4°C at 150,000 × *g*, using a TH 641 swing-out rotor in a Sorvall OTD-COMBI ultracentrifuge (Sorvall, Wilmington, Del.). Finally, the sucrose gradients were fractionated (0.55-ml fraction size) by pumping from the bottom with a capillary and a peristaltic pump. The protein concentration was monitored at 280 nm with a single-path monitor UV1 (Pharmacia, Uppsala, Sweden) and fractions were collected with a FRAC 100 fraction collector (Pharmacia). Every third fraction was checked by transmission electron microscopy for the presence and number of strands. Fractions containing strands were analyzed by sodium dodecyl sulfate (SDS)-polyacrylamide gel electrophoresis (PAGE), by the method of Laemmli (24), with a 10% (vol/vol) slab gel. The gel was fixed in 50% (vol/vol) methanol overnight and then silver stained for protein and lipopolysaccharide (LPS) detection by the method of Wray et al. (39).

Freeze-fracture replication of *M. fulvus*. Cells in mid-log phase were sedimented from the culture medium by centrifugation for 3 min at 7,000 × *g* (Hettich Ultra Rapid, Hettich, Tuttlingen, Germany) at ambient temperature. The supernatant was discarded and the vessel wall was carefully drained with filter paper, in order to prevent resuspension of the sedimented cells. Cells were picked up with a 50-μl glass capillary, and a volume of 3 to 5 μl was applied to a specimen holder. The samples were shock frozen at 89.3 K by plunging them into melting ethane. Frozen samples were stored in liquid nitrogen until further use.

Frozen samples were transferred into a freeze-fracture unit (BAF 400T, Balzers Union, Liechtenstein) at 153 K. After setting the temperature to 173 K and temperature equilibration the samples were fractured with a rotating knife. Sublimation was done at a vacuum pressure of 2×10^{-5} Pa at 173 K for 120 s. Replication was done by platin/carbon evaporation with an electron gun under a 25° elevation angle, followed by carbon backing at 90°. Replicas were cleaned by floating on sodium hypochlorite (~13% active chlorine) and incubation overnight at ambient temperature. Replicas were washed three times by floating on distilled water for each 30 min and then further cleaned with 60% (vol/vol) sulfuric acid for 3 to 6 h at ambient temperature. After three final washes on distilled water for 30 min each, the replicas were picked up with formvar-coated grids and blotted with filter paper. The dried replicas were analyzed by transmission electron microscopy.

Electron microscopy. Aliquots of disintegrated cell walls and of sucrose-gradient purified strands were diluted with HEPES-NaCl buffer to a final concentration of 60 to 80 μg of protein per ml, adsorbed to carbon-Collodion foils on 300-mesh copper grids, and drained from bulk volume without drying. The grids were negatively stained with freshly prepared 4% (wt/vol) aqueous uranylacetate for 1 s on a drop of stain solution, blotted with filter paper, and then air dried. Electron microscopy was done with a transmission electron microscope EM 10B (Zeiss, Oberkochen, Germany) or with an energy-filtered transmission electron microscope CEM 902 (Zeiss, Oberkochen, Germany) at 80 to 85 kV acceleration voltage in a magnification range from ×7,000 to ×40,000.

RESULTS

Macromolecular morphology. After gentle mechanical disruption of *M. xanthus* DK1622 and Mx x48 and treatment of the collected cell wall fragments with lysozyme chain-like aggregates, so-called strands were released from the bacterial cells (Fig. 1a and b). These strands appear in patchlike fragments of the so-called belt, the supposed final organizational state of this part of the gliding machinery (for nomenclature, see reference 25). These fragments show a characteristic cross-striation with a spacing of 16.6 ± 1.1 nm (n = 59) for strain Mx x48 (Fig. 1a) and 15.5 ± 0.6 nm (n = 41) for strain DK1622 (Fig. 1b). The ring elements show an outer diameter ranging

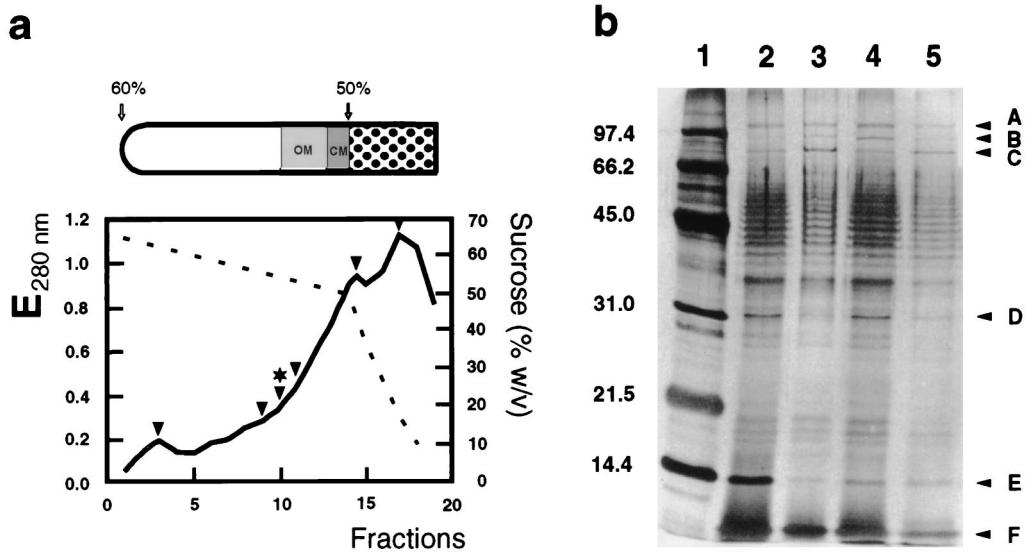

FIG. 2. Purification and biochemical characterization of chain-like strands from *M. xanthus* Mx x48. (a) Enrichment of strands by isopycnic sucrose density gradient centrifugation. The gradient range and banding of outer membrane (OM) and cytoplasmic membrane (CM) in the tube is indicated (sucrose cushion is not included). The dashed line shows the profile of the sucrose gradient after the run; arrowheads mark gradient fractions, which were analyzed by transmission electron microscopy; the asterisk indicates the fraction, which was analyzed by SDS-PAGE. (b) SDS-PAGE of different stages of the enrichment protocol. Lanes: 1, molecular mass standards as indicated at the left; 2, crude cell wall after lysozyme treatment; 3, fraction of the sucrose density gradient indicated by asterisk in panel a; 4, sediment fraction of pooled sucrose gradient samples; 5, concentrated supernatant of pooled sucrose gradient fractions. Bands A (99 kDa), B (90 kDa), and D (31 kDa) represent protein masses associated with the outer membrane vesicle fraction; band C (82 kDa) is a strand-associated protein; band E is residual lysozyme; band F represents lipid A; the ladder pattern between C and D is the LPS, typically stained by silver stain.

from 16.6 ± 1.0 nm (n = 55) for strain Mx x48 to 16.4 ± 1.5 nm (n = 37) for DK 1622.

As is seen from the insets in Fig. 1a and b with both *M. xanthus* strains, the ring elements of the strands are composed of six to seven peripheral globular masses, arranged in a circle, while the central area occasionally shows three spoke-like elements (arrows). The ring elements are equidistant and connected by two fibrillar, so-called elongated elements, indicated by dots, which run parallel at a distance of about 5.5 nm.

Isolation and biochemical characterization. Systematic studies on the release of strands from *M. xanthus* showed that these complex superstructures are rather sensitive against treatment with even mild detergents, like polyoxyethylen-10-tridecyl-ether (POE) or Triton X114. For instance, it was found that solubilization of cells with 0.5% POE led to a satisfactory disintegration of the bacterial membranes. However, this resulted in a virtually quantitative destruction of the chain-like aggregates. The highest detergent concentration to be tolerated by the strands was 0.3% POE. But with this detergent concentration the cell membranes could not be adequately solubilized.

Various methods were tested to disrupt the cells mechanically, such as French press, ultrasound, and glass bead milling. Only the French press led to acceptable results. Further, it turned out to be important to maintain the ionic strength of 0.1 mol of NaCl per liter to prevent rapid dissociation of the macromolecular complexes. Under these conditions the strands could be stored for 4 to 6 days at 4°C.

It was found that the amount of strands could be raised significantly when the crude cell wall preparation was incubated for at least 90 min with 1 mg of lysozyme per ml. Centrifugation at 17,000 × g for 30 min sedimented most of the strands and their aggregates. This material was used for further purification.

The following separation procedures were tested: gel exclusion chromatography, ion-exchange chromatography, matrix-free isoelectric focusing, and isopycnic centrifugation on sucrose gradients. Using a combination of step and linear density sucrose gradients led to a significant separation of crude cell membrane fragments and strands (see Fig. 3a). By electron microscopic examination of gradient fractions, individual chain-like aggregates were found enriched at boyant densities from 1.21 to 1.23 g/cm^3 as a broad, bright orange band (Fig. 2a). A second intense orange band appeared at lower density, between 1.19 and 1.21 g/cm^3. However, electron microscopic analysis demonstrated only membrane material, i.e., fragments of the cytoplasmic membrane, and no strand morphologies were recognized. The sediment mainly contained crude cell wall fragments, associated with clumps of amorphous matter. This slime-like material entrapped varying amounts of chain-like aggregates, which explains their nonquantitative yield.

The final purification step was a differential centrifugation of the pooled 1.21- to 1.23-g/cm^3 density bands, diluted to 11% (wt/vol) sucrose in HEPES-saline buffer. As can be seen in Fig. 3b, the sediment mainly consisted of vesicles and fragments of the outer membrane. Only trace amounts of strands were present, while in the supernatant the strands were significantly enriched (Fig. 3c).

Characterization of the chain-like aggregates by SDS-PAGE. The polypeptide composition of the material after the different purification steps was characterized by SDS-PAGE on silver-stained gels (Fig. 2b). The crude cell wall material containing strands (lane 2) is mainly characterized by bands A, C, D, and E, further by the characteristic LPS pattern between 40 and 60 kDa, and lipid A (band F). Band E (14.4 kDa) represents lysozyme, carried along the purification procedure. Of the high-molecular-mass polypeptides A (99.0 kDa), B (90.0 kDa), and C (82.0 kDa), only polypeptide C appears to be enriched in the supernatant and thus may be associated with the strands (Fig. 2b, lane 5). Lane 3 represents the pooled gradient fractions 9 and 10. The corresponding sediment fraction, viz., lane 4, clearly shows a higher proportion of LPS

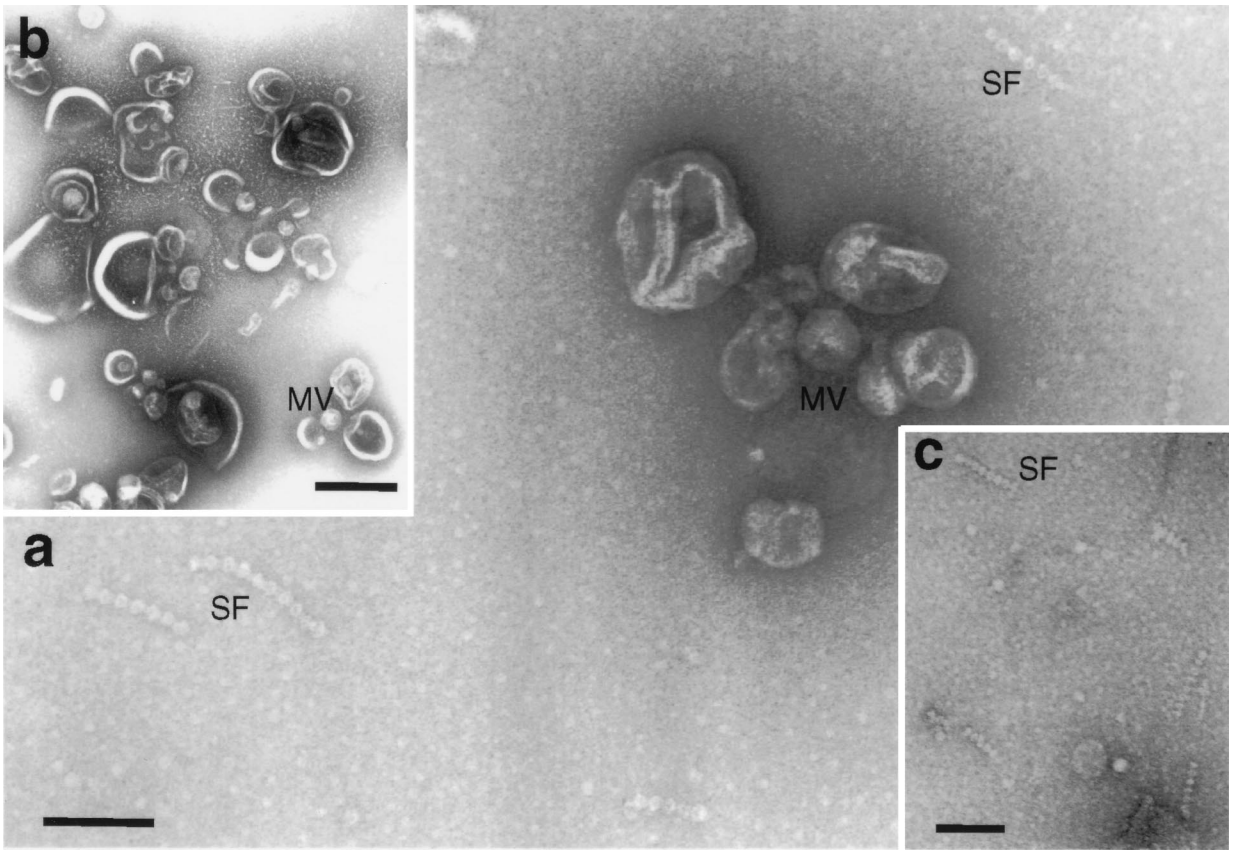

FIG. 3. Electron microscopic analysis of enriched strand fractions. (a) Pooled fraction of strand-enriched samples from a sucrose gradient at 1.21-g/cm^3 density. (b) Sediment fraction of differentially centrifuged pooled fractions from panel a, containing mainly membrane vesicles (MV). (c) The corresponding supernatant enriched with strand fragments (SF). Bars, 100 nm (a), 200 nm (b), 100 nm (c).

molecules, which is in accordance with the electron microscopic results (Fig. 3b). This fraction is mainly composed of membrane vesicles, which have to be interpreted as outer membrane residues because of their characteristic LPS pattern, their shape, and their density (1.22 g/cm^3). The polypeptides A, B, and D are enriched relative to the concentrated supernatant fraction; thus, these polypeptides appear to be outer membrane associated. Still, outer membrane constituents have not been completely removed from the supernatant (Fig. 2b, lane 5), although they are drastically reduced relative to the sediment fraction (Fig. 2b, lane 4). These results are in agreement with the corresponding electron microscopic analysis of these samples (see Fig. 3b and c).

Electron microscopic observation of the chain-like aggregates in situ. Electron microscopy shows the strands to be directly associated or fixed to a membrane-like substratum of strain Mx x48. In Fig. 4b several chain-like aggregates run parallel along the membraneous surface. For instance, two chains can be observed in the inset of Fig. 4b, indicated by solid triangles. They appear to be in a perpendicular position relative to the surface. The ring elements have an outer diameter between 12.4 and 14.0 nm and are at a distance of 12.4 to 14.0 nm in the case of *M. xanthus* Mx x48.

Physical fixation of bacteria by quick freezing in an appropriate coolant arrests physiological and dynamic states. With the freeze-fracture technique it was possible to get a topographic relief-like view from parts of the myxococcal cell wall after brief sublimation of the frozen fractured sample surface and replication as it is shown in Fig. 4a. In this case details of the molecular organization of the cell wall of *M. fulvus* Mx f65/9, could be observed. Ring elements were found within the periplasmic space of the gram-negative cell wall near the apical end of an individual cell (Fig. 4a). During the sublimation process, ice surrounding the bacterial surface was removed and the topography of the cell surface was thus set free. A narrow rim of the outermost layer, i.e., the surface of the outer membrane, could be examined (Fig. 4a, c, and d). As can be seen in detail, semicircular structures emerge from this surface about 5.6 nm in height and they appear to be aligned in a similar way as the negatively stained ring elements of the chain-like aggregates (semicircular ring elements [RE] are indicated in Fig. 4c). From this perspective the semicircular structures have a spacing of about 7.5 nm. Within the periplasmic space, which measures 23 to 29 nm in width (Fig. 4c and d), individual ring elements can be recognized (Fig. 4d, inset). They appear to be composed of six to seven peripheral protein masses and a central protein mass and have an outer diameter of 11.2 to 13.0 nm. The position of these ring-like molecules within the periplasmic space is the outer half, i.e., the space outside the central murein layer and the inner surface of the outer membrane. Our morphological data on the in situ organization of the chain-like strands, observed in *M. fulvus* as well as *M. xanthus* vegetative cells, are summarized in a three-dimensional (3D) model (Fig. 5; 3D-model not drawn to scale).

DISCUSSION

The present paper describes in detail chain-like aggregates, so-called strands, within the cell wall of two strains of *M. xanthus*. Macromolecular structures isomorphic with those de-

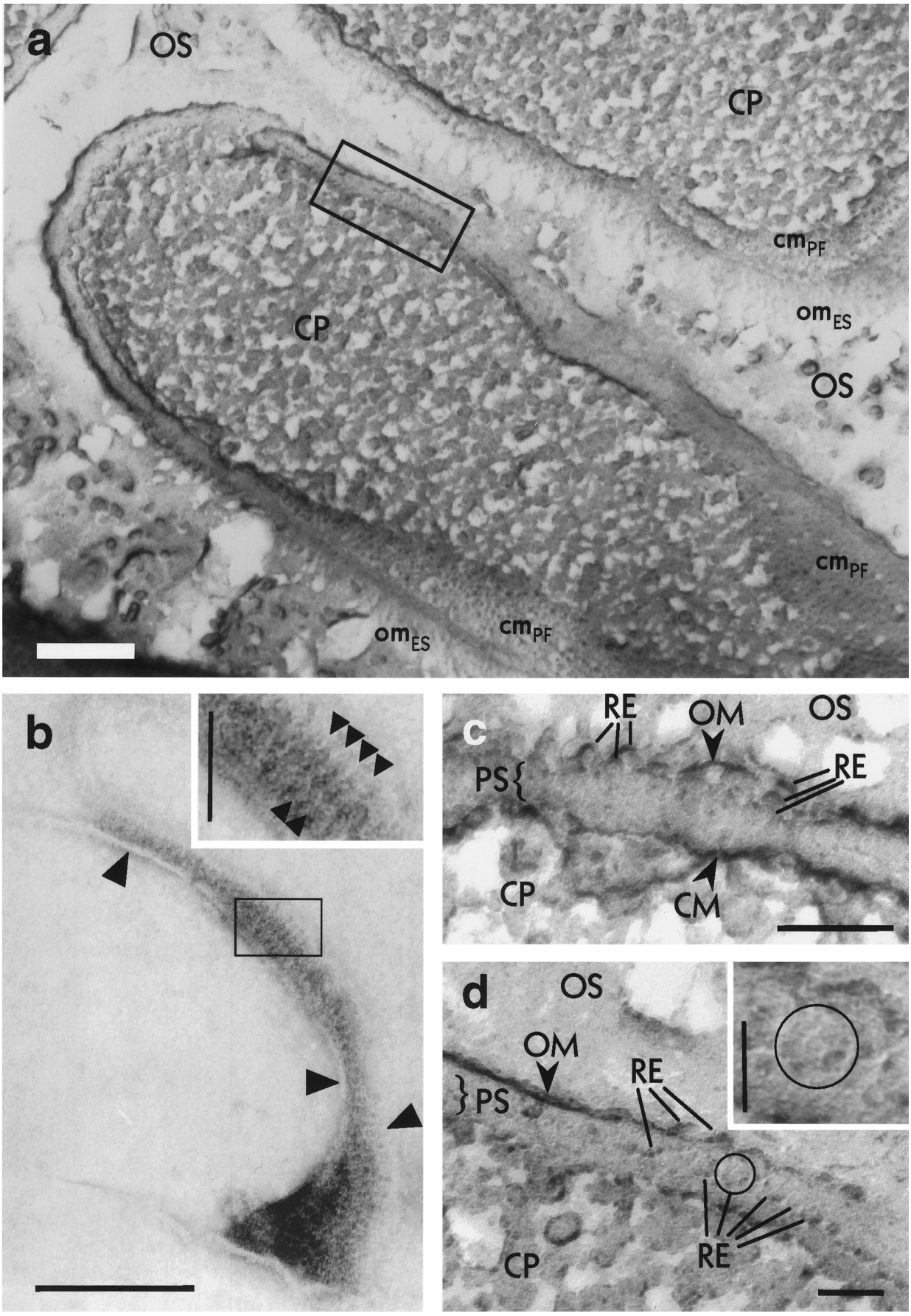
a
OS
CP
CP
cm PF
om ES
OS
cm PF
om ES
cm PF
b
c
RE
OM
OS
PS{
RE
CP
CM
d
OS
OM
RE
} PS
CP
RE

FIG. 4. Electron microscopic analysis of in situ localization of macromolecular structures of *Myxococcus* spp., isomorphic with negatively stained chain-like strands. (a) Survey of freeze-fractured vegetative cells of *M. fulvus*. The frame indicates the cell wall area shown in detail in panel d. CP, cytoplasm; OS, outer space; cm_{PF}, plasma fracture face of the cytoplasmic membrane; om_{EF}, external face of the outer membrane surface. Bar, 150 nm. (b) Negatively stained fragment of a membrane lobe of *M. xanthus* Mx x48. Solid triangles point to the rim of underlaying membrane layer. Aligned chain-like strands are associated with it and are standing normal to the membrane. Inset: Detail view of strands, framed in panel b; individual ring elements are indicated by triangles. Bar: 125 nm (inset, 45 nm). (c and d) Details of freeze-fractured cell walls of *M. fulvus*. Individual ring elements (RE), parts of the chain-like strands, are indicated and shown enlarged in the inset in panel d. The linear arrangement of ring elements, partially contouring the cell surface, is shown in panel c. OS, outer space; OM, outer membrane; CM, cytoplasmic membrane; PS, periplasmic space. Bars: 50 nm (c); 40 nm (d).

scribed here have recently been reported from *M. fulvus*. Isolated superstructures of the strands, so-called ribbons, showed a remarkable conformational flexibility, which was believed to be the basis for the mechanics of gliding motility of this bacterium (25). These strands and their more complex aggregates, i.e., the ribbons and the belt, were assumed to be the underlying principle of a distinct surface pattern found with negatively stained mid-log-phase cells running helically around the apical end of the myxococcal cell. This surface pattern showed significant ultrastructural and spatial homologies to the dimensions observed on the isolated strands and ribbons.

The formerly made assumption that the strands and their aggregates are near the outer surface and integrated within the periplasmic space can now be substantiated by the following observations. (i) The strands stick tightly to membrane-like fragments, which by buoyant density and LPS pattern in PAGE represent the outer membrane. This association appears to be the original functional state. (ii) The biochemical data are supported by electron microscopic observations, which show the strands in close connection with a membrane-like planar layer. (iii) Freeze-fracturing cells allows study of their actual morphological and physiological state. In *M. fulvus* freeze-fracture replicas, ring-like elements were found within the periplasmic space and in tight contact with the outer membrane. The rings had an outer diameter of 11.2 to 13 nm and consisted of six to seven peripheral protein masses and one central protein mass. Multiples of them appeared to be aligned within the periplasmic space and represented thus the morphological equivalents of the strands. These ring-like elements were seen normal to the plane of the outer membrane and determined to a certain degree the microtopography of the bacterial outer surface (Fig. 4a, c, and d). While the outer diameter of the ring elements, when measured from freeze-fracture replicas, was about 15% smaller than in negatively stained samples, this can be explained by different projection angles of the ring elements relative to the electron beam. Thus the in situ ultrastructural data are in good agreement with the observations on negatively stained preparations of dislocated aggregates and further corroborate that at least part of the supposed machinery of gliding motility is located immediately under the outer membrane.

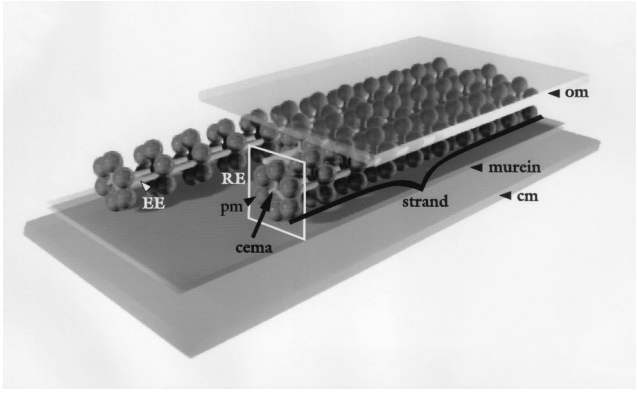

FIG. 5. 3D model of the location of strands within the cell wall of *Myxococcus* spp. As part of the belt, three strands are presented. They represent the periplasmic part of the gliding motility apparatus. These strands are inserted between the highly flexible murein sacculus and the outer membrane. Only that conformational state of the ring elements in which they are standing normal to the outer membrane plane is shown. Model not drawn to scale. RE, ring element, framed; EE, elongated element; CM, cytoplasmic membrane; OM, outer membrane; cema, central mass; pm, peripheral mass.

One may speculate about how the machinery is energized in order to fulfill locomotion by coordinated conformational changes of the ring elements along the strands, as it has been proposed by Lünsdorf and Reichenbach (25). It has been shown repeatedly and for various microorganisms that gliding movement is driven directly by the proton motive force and is independent from ATP (4, 14, 17, 19, 28, 34). Thus, the energy has to be transmitted to the strands in order to induce in this macromolecular ensemble a possibly synchronized wave of conformational changes in an until now unknown manner (for details on the conformational flexibility of the strands, see reference 25). Further, the morphological data indicate that this superstructure is sandwiched between the outer membrane and the murein sacculus. On electron micrographs the murein sacculus can be seen as an isolated continuum. It appears to be rather flaccid (data not shown) and is believed not to hinder conformational changes along the strands.

The present morphological data are clearly in contradiction to the model of the gliding machinery based on rotary assemblies within the cytoplasmic membrane described for *Flexibacter columnaris*. In this model, the energy and force vectors needed for locomotion are directly transferred to the outer surface (28–30). If the rotary assemblies were the structural equivalents to the flagellar motors as suggested, they would have to be located within the cytoplasmic membrane, as has been claimed by Rowbury et al. (35). They would represent the counterparts of the M and S rings of the flagellar motor (12, 20, 26) and thus should be seen as characteristic features within the cytoplasmic membrane of freeze-fracture replicas as was shown for the polar flagellar tufts of *Aquaspirillum serpens* (10) and single flagella of *Salmonella thyphimurium* (23). No gliding bacteria that have been studied by freeze-fracture replication, i.e., *Cytophaga aquatilis* and *Cytophaga johnsonae* (38), *Cytophaga columnaris* and *Myxococcus xanthus* (5), *Cytophaga* spp. (2), and the present study on *M. fulvus*, showed ultrastructural details within the cm_{PF} plane which resembled the M and S rings of the flagellar motor.

The localization of the strands within the periplasm between the outer membrane and the murein continuum implies a rather different ultrastructural and macromolecular organization of the gliding machinery of *Myxococcus*, as this supposed part of the gliding apparatus obviously is not integrated within the cytoplasmic membrane. From this point of view, the strands and on the whole the belt represent a kind of periplasmic mechanoprotein construction, which may be energized via still unknown linkers of the membrane potential, thus inducing coordinated conformational changes of the strands. The obvi-

ously tight association of the strands with the outer membrane should allow mechanical energy to be transmitted from the supposed apparatus of gliding motility to the outer surface of the cell, e.g., in the form of a contraction wave, and thus drive the cell forward. The energy needed for the conformational changes could be gained and generated directly by transcellular power transmission by $\Delta\psi$, i.e., the transmembrane electric potential difference, as it is proposed by Chailakhyan et al. (9) in their electrical cable model on power transmission along gliding trichomes of the cyanobacterium *Phormidium uncinatum*. In the case of *Myxococcus* motility, coordination and tactic behavior would still be under the control of the frz-signal transduction system (for reviews, see references 27 and 40).

The presented in situ localization of the chain-like strands in direct contact to the outer membrane within the periplasm implies a dichotomic organization of the gliding apparatus in toto. This kind of organization may be easily extended to filamentous gliding bacteria, i.e., cyanobacteria, *Flexibacter*, *Herpetosiphon*, *Thioploca*, and others. Here a coordinated transcellular power transmission of $\Delta\psi$ of individual protoplasts may establish continuous gliding motility. Further work on the isolation of structural elements of the strands and their biochemical characterization is in progress, thus opening the possibility for immunocytochemical labelling of individual motility elements.

The apparent ultrastructural complexity of the chain-like aggregates opens further questions on their biosynthesis and exportation into the periplasm and its insertion between outer membrane and murein sacculus, as well as on the organization of that part of the gliding apparatus, which is supposed to be associated with the cytoplasmic membrane, and its macromolecular integration.

ACKNOWLEDGMENTS

The skillful technical assistance of Elke Haase is gratefully acknowledged. We thank D. Kaiser, Department of Biochemistry/Developmental Biology, Stanford University, for making *M. xanthus* DK 1622 available to us.

REFERENCES

1. **Agnihothrudu, V., G. C. S. Barua, and K. C. Barua.** 1959. Occurrence of *Chondromyces* in the rhizosphere of plants. Indian Phytopathol. **12:**158–160.
2. **Beatson, P. J., and K. C. Marshall.** 1994. A proposed helical mechanism for gliding motility in three gliding bacteria (order *Cytophagales*). Can. J. Microbiol. **40:**173–183.
3. **Burchard, R. P.** 1981. Gliding motility of prokaryotes: ultrastructure, physiology, and genetics. Annu. Rev. Microbiol. **35:**497–529.
4. **Burchard, R. P.** 1984. Gliding motility and taxes, p. 139–1161. *In* E. Rosenberg (ed.) The myxobacteria. Springer Verlag, Heidelberg, Germany.
5. **Burchard, R. P., and D. T. Brown.** 1973. Surface structure of gliding bacteria after freeze-etching. J. Bacteriol. **114:**1351–1355.
6. **Burnham, J. C., S. A. Collart, and B. W. Highison.** 1981. Entrapment and lysis of the cyanobacterium *Phormidium luridum* by aqueous colonies of *Myxococcus fulvus* PC 02. Arch. Microbiol. **129:**285–294.
7. **Burnham, J. C., S. A. Collart, and M. J. Daft.** 1984. Myxococcal predation of the cyanobacterium *Phormidium luridum* in aqueous environments. Arch. Microbiol. **137:**220–225.
8. **Castenholz, R. W.** 1982. Motility and taxes, p. 413–439. *In* N. G. Carr and B. A. Whitton (ed.), The biology of cyanobacteria. Blackwell Scientific Publications, Oxford, United Kingdom.
9. **Chailakhyan, L. M., A. N. Glagolev, T. N. Glagoleva, G. V. Murvanidze, T. V. Potapova, and V. P. Skulachev.** 1982. Intercellular power transmission along trichomes of cyanobacteria. Biochim. Biophys. Acta **679:**60–67.
10. **Coulton, J. W., and R. G. E. Murray.** 1978. Cell envelope associations of *Aquaspirillum serpens* flagella. J. Bacteriol. **136:**1037–1049.
11. **Daft, M. J., J. C. Burnham, and Y. Yamamoto.** 1985. Lysis of *Phormidium luridum* by *Myxococcus fulvus* in continuous flow cultures. J. Appl. Bacteriol. **59:**73–80.
12. **DePamphilis, M. L., and J. Adler.** 1971. Fine structure and isolation of the hook-basal body complex of flagella from *Escherichia coli* and *Bacillus subtilis*. J. Bacteriol. **105:**384–395.
13. **Doetsch, R. N., and G. J. Hageage.** 1968. Motility in procaryotic organisms: problems, points of view, and perspectives. Biol. Rev. **43:**317–362.
14. **Duxburry, T., B. A. Humphrey, and K. C. Marshall.** 1980. Continuous observations of bacterial gliding motility in a dialysis microchamber: the effects of inhibitors. Arch. Microbiol. **124:**169–175.
15. **Dworkin, M.** 1996. Recent advances in the social and developmental biology of the myxobacteria. Microbiol. Rev. **60:**70–102.
16. **Fossing, H., V. A. Gallardo, B. B. Jørgensen, M. Hüttel, L. P. Nielsen, H. Schulz, D. E. Canfield, S. Forster, R. N. Glud, J. K. Gundersen, J. Küver, N. B. Ramsing, A. Teske, B. Thamdrup, and O. Ulloa.** 1995. Concentration and transport of nitrate by the mat-forming sulphur bacterium *Thioploca*. Nature **374:**713–715.
17. **Glagoleva, T. N., A. N. Glagolev, M. V. Gusev, and K. A. Nikitina.** 1980. Protonmotive force supports gliding in cyanobacteria. FEBS Lett. **117:**49–53.
18. **Häder, D. P.** 1987. Photosensory behavior in procaryotes. Microbiol. Rev. **51:**1–21.
19. **Halfen, L. N., and R. W. Castenholz.** 1971. Gliding motility in the blue-green alga *Oscillatoria princeps*. J. Phycol. **7:**133–145.
20. **Jones, C. J., M. Homma, and R. M. Macnab.** 1989. L-, P-, and M-ring proteins of the flagellar basal body of *Salmonella typhimurium*: gene sequences and deduced protein sequences. J. Bacteriol. **171:**3890–3900.
21. **Kaiser, D., C. Manoil, and M. Dworkin.** 1979. Myxobacteria: cell interactions, genetics and development. Annu. Rev. Microbiol. **33:**595–639.
22. **Kaiser, D., and L. Kroos.** 1993. Intercellular signaling, p. 257–2283. *In* M. Dworkin and D. Kaiser (ed.) Myxobacteria II. American Society for Microbiology, Washington, D.C.
23. **Khan, S., I. H. Khan, and T. S. Reese.** 1991. New structural features of the flagellar base in *Salmonella typhimurium* revealed by rapid-freeze electron microscopy. J. Bacteriol. **173:**2888–2896.
24. **Laemmli, U. K.** 1970. Cleavage of structural proteins during the assembly of the head of bacteriophage T4. Nature **227:**680–685.
25. **Lünsdorf, H., and H. Reichenbach.** 1989. Ultrastructural details of the apparatus of gliding motility of *Myxococcus fulvus* (Myxobacterales). J. Gen. Microbiol. **135:**1633–1641.
26. **Macnab, R. M., and D. J. DeRosier.** 1988. Bacterial flagellar structure and function. Can. J. Microbiol. **34:**442–451.
27. **McBride, M. J., P. Hartzell, and D. R. Zusman.** 1993. Motility and tactic behavior of *Myxococcus xanthus*, p. 285–305. *In* M. Dworkin and D. Kaiser (ed.), Myxobacteria II. American Society for Microbiology, Washington, D.C.
28. **Pate, J. L., and L. Y. E. Chang.** 1979. Evidence that gliding motility in procaryotic cells is driven by rotary assemblies in the cell envelopes. Curr. Microbiol. **2:**59–64.
29. **Pate, J. L.** 1985. Gliding motility in *Cytophaga*. Microbiol. Sci. **2:**289–295.
30. **Pate, J. L.** 1988. Gliding motility in procaryotic cells. Can. J. Microbiol. **34:**459–465.
31. **Reichenbach, H.** 1981. Taxonomy of the gliding bacteria. Annu. Rev. Microbiol. **35:**339–364.
32. **Reichenbach, H., and M. Dworkin.** 1992. The myxobacteria, p. 3416–3487. *In* A. Belows, H. G. Trüper, M. Dworkin, W. Harder, and K.-H. Schleifer (ed.), The Procaryotes, 2nd ed. Springer Verlag, Heidelberg, Germany.
33. **Reichenbach, H.** 1993. Biology of the myxobacteria: ecology and taxonomy, p. 13–62. *In* M. Dworkin and D. Kaiser (ed.), Myxobacteria II. American Society for Microbiology, Washington, D.C.
34. **Ridgway, H. F.** 1977. Source of energy for gliding motility in *Flexibacter polymorphus*: effects of metabolic and respiratory inhibitors on gliding movement. J. Bacteriol. **131:**544–556.
35. **Rowbury, R. J., J. P. Armitage, and C. King.** 1983. Movement, taxes and cellular interactions in the response of microorganisms to the natural environment, p. 299–350. *In* J. H. Slater, R. Whitenbury, and J. W. T. Wimpenny (ed.), Microbes in their natural environments. Cambridge University Press, Cambridge, United Kingdom.
36. **Shimkets, L. J.** 1990. Social and developmental biology of the myxobacteria. Microbiol. Rev. **54:**473–501.
37. **Stackebrandt, E.** 1985. Phylogeny and phylogenetic classification of procaryotes, p. 309–334. *In* K. H. Schleifer and E. Stackebrandt (ed.), Evolution of prokaryotes (FEMS Symposium 29). Academic Press, London, United Kingdom.
38. **Strohl, W. R.** 1979. Ultrastructure of *Cytophaga johnsonae* and *C. aquatilis* by freeze-etching. J. Gen. Microbiol. **112:**261–268.
39. **Wray, W., T. Boulikas, V. P. Wray, and R. Hancock.** 1981. Silver staining of proteins in polyacrylamide gels. Anal. Biochem. **118:**197–203.
40. **Zusman, D. R., and M. J. McBride.** 1991. Sensory transduction in the gliding bacterium *Myxococcus xanthus*. Mol. Microbiol. **5:**2323–2329.